

## Competing phases in the high field phase diagram of $(\text{TMTSF})_2\text{ClO}_4$

S. Haddad<sup>1</sup>, S. Charfi-Kaddour<sup>1</sup>, C. Nickel<sup>2</sup>, M. Héritier<sup>2</sup> and R. Bennaceur<sup>1</sup>

<sup>1</sup> *Laboratoire de Physique de la Matière Condensée, Département de Physique, Faculté des Sciences de Tunis, Campus universitaire 1060 Tunis, Tunisia*

<sup>2</sup> *Laboratoire de Physique des Solides (associé au CNRS), Université de Paris-Sud 91405 Orsay, France*

A model is presented for the high field phase diagram of  $(\text{TMTSF})_2\text{ClO}_4$ , taking into account the anion ordering, which splits the Fermi surface in two bands. For strong enough field, the largest metal-SDW critical temperature corresponds to the  $N=0$  phase, which originates from two intraband nesting processes. At lower temperature, the competition between these processes puts at disadvantage the  $N=0$  phase vs. the  $N=1$  phase, which is due to interband nesting. A first order transition takes then place from the  $N=0$  to  $N=1$  phase. We ascribe to this effect the experimentally observed phase diagrams.

PACS numbers: 64.60.-i, 64.60.Ak, 72.15.Gd, 71.10.Pm, 74.70.Kn, 75.30.Fv

The Bechgaard salts,  $(\text{TMTSF})_2\text{X}$ , ( $\text{X} = \text{PF}_6, \text{ClO}_4, \text{ReO}_4\dots$ ) exhibit a rich variety of original properties [1]. One of the most interesting phenomena is certainly the quantum cascade of Spin Density Wave (SDW) phases induced by a magnetic field. The simplest case is given by the  $\text{X}=\text{PF}_6$  salt. In the low temperature metallic phase of this salt, a moderate magnetic field applied in a direction perpendicular to the most conducting planes induces a cascade of transitions to SDW phases, exhibiting the quantized Hall resistance  $\rho_{xy} = h/2Ne^2$  in the sequence  $N = \dots, 5, 4, 3, 2, 1, 0$  as the field is increased. The experimental data are well explained by the Quantized Nesting Model (QNM) [2–6]: in a Fermi liquid approach of the metallic phase, described by two slightly warped parallel sheets Fermi surface, the orbital effect of the magnetic field destabilizes the metal by inducing a sort of Peierls instability to a SDW phase. As the field is varied, the SDW wave vector adjusts itself to ensure the Peierls condition that the Fermi level lies in the middle of one of the SDW Landau gaps.

While the experiments in the  $\text{PF}_6$  salt are well explained, even with a quite simple Fermi surface model, the case of the  $\text{ClO}_4$  salt exhibits distinct deviations from the  $\text{PF}_6$  behavior which, definitely, cannot be understood within the QNM [7–13]. Although the phenomenon of quantized cascade of SDW phases still exists, the phase diagram is more complex. In the  $\text{ClO}_4$  salt, the quantized cascade is observed up to 8 T. When the magnetic field  $H$  is further increased, the metal-SDW second order transition temperature continues to increase smoothly, but saturates at about 5.5 K for  $H$  larger than 18 T. In contrast with the behavior of the  $\text{PF}_6$  salt, a second phase transition occurs inside the domain of stability of the field induced SDW. This is a first order transition, with a maximum transition temperature of 3.5 K for  $H = 20$  T. When  $H$  is increased above 20 T, this transition temperature strongly decreases and vanishes at 28 T. The existence of this first order line for  $20 \text{ T} < H < 28 \text{ T}$  has

been first reported by McKernan *et al.* [9]. J. Moser [12] has proposed that this line should be prolonged for  $17 \text{ T} < H < 20 \text{ T}$  with a transition temperature strongly decreasing as  $H$  decreases from 20 T to 17 T, which has been confirmed recently by Chung *et al.* [13]. The labeling of the field induced phases by a definite quantum number  $N$  is by no means obvious in this high field part of the phase diagram. Below 0.3 K, a quantized Hall plateau, corresponding to  $N=1$  phase has been observed for  $8 \text{ T} < H < 28 \text{ T}$ . The first order transition at  $H = 28$  T and low temperature leads to a highly resistive state, with a non quantized Hall resistance, which is strongly reminiscent of a  $N=0$  SDW phase [7,9]. These two facts would seem to imply the values of the quantum number  $N$  in the  $(H, T)$  plane, since  $N$  cannot change unless a first order transition line is crossed. These experimental evidences are at variance with several previous theoretical works, predicting a "metallic reentrance" as a consequence of the QNM.

Many authors [14–16] have proposed to ascribe the different behavior of the  $\text{ClO}_4$  salt to the existence of an ordering of the perchlorate anions, which occurs at 24 K. This dimerizes the system along the  $\mathbf{b}$  direction and opens a gap in the original two-sheet Fermi surface, giving rise to four open sheets of Fermi surfaces.

In this paper, we propose a model to describe properly the behavior of the  $\text{ClO}_4$  salt. Although the starting point of this work is a generalization of the QNM, new ingredients are introduced which are substantially important in the determination of the phase diagram. In particular, two main ideas, completely neglected so far, turn out to be decisive: (i) the renormalization of the electron-electron scattering strengths by the low dimensional fluctuations is different for different SDW phases. (ii) the competition between a usual single wave vector SDW phase and an original SDW phase characterized by two coupled order parameters, which do not compete but on the contrary cooperate to stabilize this phase. These

ideas have not been already discussed in the literature. The resulting features deduced from our model are consistent with the experimental observations listed above, but quite different from that of previous works [14–16].

As in the standard QNM, we approximate the quasi-1D spectrum of Bechgaard salts, when no anion ordering is present, by a two harmonics dispersion relation:

$$\epsilon(\vec{k}) = v_F (|k_x| - k_F) - 2t_1 \cos k_y b - 2t_2 \cos 2k_y b$$

where  $k_x$  and  $k_y$  are the electron momenta along and across the chains,  $v_F$  is the Fermi velocity and  $b$  is the interchain distance.  $t_1$  denotes the effective interchain transfer integrals to nearest neighbors, and the  $t_2$  term accounts for the deviation from perfect nesting of the quasi-1D Fermi surface.

Under a magnetic field applied in the  $\mathbf{c}$  direction,  $\mathbf{H} = (0, 0, H)$  and in the Landau gauge  $\mathbf{A} = (0, Hx, 0)$ , the non interacting Hamiltonian in the absence of anion ordering takes the form

$$H_{eff}^0 = v_F \left[ \left| -i \frac{\partial}{\partial x} \right| - k_F \right] - 2t_1 \cos \left[ -ib \frac{\partial}{\partial y} + ebHx \right] - 2t_2 \cos \left[ -2ib \frac{\partial}{\partial y} + 2ebHx \right]$$

In the presence of the anion ordering, which introduces a periodic potential  $V(y) = V \cos \frac{\pi}{b} y$ , the Brillouin zone is halved in the  $k_y$  axis. In the  $\{|\psi_{k_x, l}\rangle\}$  basis, where  $|\psi_{k_x, l}\rangle$  are the eigenstates of  $H_{eff}^0$ , the matrix elements of the anion potential  $V(y)$ , considered as a perturbation, are given by (eq.2 of Ref. [17])

$$\begin{aligned} \langle \psi_{\frac{2\pi n}{L}, l} | V | \psi_{\frac{2\pi n'}{L}, l'} \rangle &= V (-1)^l J_{l-l} \left( \frac{4t_1}{v_F G} \right) \\ &\times \delta \left( n - n' + \frac{LG(l-l')}{2\pi} \right) \end{aligned} \quad (1)$$

$L$  is the length of the sample along the chain direction, the integer  $l$  is used instead of  $k_y$  [17],  $J$  is the Bessel function and  $G = ebH$ . Within a perturbative treatment to first order on  $V$ , the diagonal term with  $l = l'$  in eq.1 splits the energy spectrum of the total Hamiltonian into two subbands  $E^A$  and  $E^B$  given by (see Fig.1):  $E_k^m = v_F (|k_x| - k_F^m)$ , with  $m = A, B$  and  $k_F^A = k_F - \frac{\Delta}{v_F}$  and  $k_F^B = k_F + \frac{\Delta}{v_F}$ , where  $\Delta = V J_0 \left( \frac{4t_1}{v_F G} \right)$ .

Considering  $V J_0 \left( \frac{4t_1}{v_F G} \right)$  as a perturbation is justified by an intensive experimental study [18,19], which yields a value of  $V \sim T_{AO}/2 \sim 12$  K. However, some magnetoresistance (MR) measurements [20] have led to somewhat larger estimates for  $V$ , but in fairly broad range, because of a lack of consistent interpretation of MR properties: some of them are of the order of  $t_1$  [20], others are  $\sim 50$  K [21]. Therefore,  $V$  cannot be estimated without ambiguities and difficulties [22,23]. It should be stressed that

recent theoretical studies suppose that  $V$  may be large ( $V \sim t_1$ ) [24]. Nevertheless, such values, because of a too large departure from perfect nesting, cannot account neither for the FISDW cascade, nor for the quantum Hall effect observed in  $(\text{TMTSF})_2\text{ClO}_4$ . Indeed, if  $V \sim t_1$ , the quantum Hall numbers have to be quite large ( $N \sim 50$  for  $H \sim 10$  T), in disagreement with the experimental data.

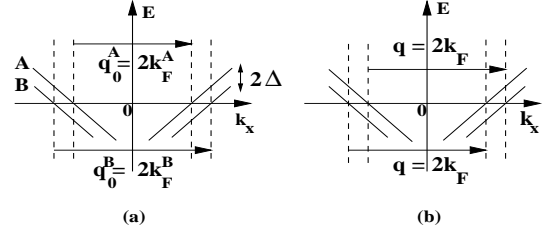


Fig.1: Band structure of quasi-1D electron system in presence of anion ordering.  $q_0^A$  and  $q_0^B$  are intraband nesting vectors respectively in the A band and the B band while  $q$  corresponds to the interband nesting vector.

The four sheets of the split Fermi surface determine, now, four different nesting processes: the intraband nesting A-A or B-B, with two different longitudinal components of the nesting vector  $q_0^A = 2k_F^A$  and  $q_0^B = 2k_F^B$ , but also the interband nesting processes A-B and B-A, with only one longitudinal component of the nesting wave vector  $q = 2k_F$ , as in the absence of anion ordering. In a Fermi liquid approach, the instability of the metallic phase is discussed by writing the Stoner criterion, which involves the non interacting spin susceptibilities. It has been shown that the formation of a SDW phase with an *even* (*odd*) value of the quantum number is associated with the divergence of the *intraband* (*interband*) susceptibilities [15]. Since we are interested in the strong field part of the phase diagram, we restrict the discussion to the phases corresponding to the two smallest quantum numbers,  $N=0$  and  $N=1$ .

The interacting part of the Hamiltonian is given by:

$$H_{int} = \frac{g_2}{2} \sum_{m_i, \sigma} \int d^2 \vec{r} \Psi(\vec{r})_{m_4, -, -\sigma}^\dagger \Psi_{m_3, +, \sigma}^\dagger(\vec{r}) \times \Psi_{m_2, +, \sigma}(\vec{r}) \Psi_{m_1, -, -\sigma}(\vec{r}) \quad (2)$$

where  $\Psi_{m_i, p, \sigma}$  denotes a fermionic operator for right ( $p = +$ ) and left ( $p = -$ ) moving particles. The band label  $m_i$  ( $i=1-4$ ) corresponds to A or B band and  $\sigma$  is the spin index. This Hamiltonian contains only the forward scattering term ( $g_2$ ). The effects of umklapp scattering ( $g_3$ ) and backward scattering ( $g_1$ ) do not play a central role in our model and will be discussed in a forthcoming paper.

For the  $N=0$  phase, we should define two order parameters since the nesting vectors of the A and the B bands are different. Let's denote by  $\Delta_0^A$  and  $\Delta_0^B$  the order parameters respectively for the A band and the B band

which are given by:  $\Delta_0^A = -\langle \Psi_{A2\uparrow}^+ \Psi_{A1\downarrow} \rangle \exp^{iq_0^A x}$  and  $\Delta_0^B = -\langle \Psi_{B2\uparrow}^+ \Psi_{B1\downarrow} \rangle \exp^{iq_0^B x}$ . We argue for the participation of the two order parameters in the stability of the N=0 phase. In fact, the possibility that only one band, A or B, is gapped at the metal-N=0 transition is not favorable to the formation of a SDW phase, since the nesting process would only involve one half of the Fermi surface density of states, which would exponentially reduce the critical temperature compared to a process involving both the A and the B bands. Involving these two bands implies the coexistence of two different SDW's wave vectors. To lowest order, each SDW has a majority component in its own band and a much smaller minority component in the other band. The two different SDW's weakly interact through this overlap of the order parameters in the same band. At the transition temperature  $T_0$  from the metallic state to N=0 phase both pairs of the Fermi surface become simultaneously gapped. The case of the N=1 phase is simpler since the stability criterion only includes interband nesting processes. In this case, the N=1 nesting involves a single wave vector  $q_1 = 2k_F + G$ , which induces the formation of a gap at the Fermi level on the four sheets of the Fermi surface. The order parameter of the N=1 phase is then given by  $\Delta_1 = -\langle \Psi_{A2\uparrow}^+ \Psi_{B1\downarrow} \rangle \exp^{iq_1 x}$ .

Based on a microscopic study, we obtain the Landau expansion of the free energy  $F_T$  of the system compared to that of the normal state  $F_{norm}$ :

$$F_T - F_{norm} = \frac{a_0}{2} (\Delta_0^A)^2 + \frac{a_0}{2} (\Delta_0^B)^2 + \frac{b_0}{2} (\Delta_0^A)^4 + \frac{b_0}{2} (\Delta_0^B)^4 + c_0 (\Delta_0^A)^2 (\Delta_0^B)^2 + a_1 (\Delta_1)^2 + b_1 (\Delta_1)^4 + \frac{d_{01}}{2} (\Delta_1)^2 \left[ (\Delta_0^A)^2 + (\Delta_0^B)^2 \right]$$

We find that the coupling term  $d_{01}$ , which is positive and fairly strong, leads to an increase of  $F_T$ . When minimizing  $F_T$  with respect to  $\Delta_0$  and  $\Delta_1$  ( $\Delta_0 \equiv \Delta_0^A = \Delta_0^B$ ), we find that the minimum free energy is not obtained when  $\Delta_0$  and  $\Delta_1$  coexist, but when either  $\Delta_0$  or  $\Delta_1$  vanishes. Then, the total free energy  $F_T$  reduces to the free energy  $F_0$  or  $F_1$  respectively of the N=0 and the N=1 FISDW phases given by:

$$F_0 - F_{norm} = \frac{a_0}{2} (\Delta_0^A)^2 + \frac{a_0}{2} (\Delta_0^B)^2 + \frac{b_0}{2} (\Delta_0^A)^4 + \frac{b_0}{2} (\Delta_0^B)^4 + c_0 (\Delta_0^A)^2 (\Delta_0^B)^2 \quad (3)$$

$$F_1 - F_{norm} = a_1 (\Delta_1)^2 + b_1 (\Delta_1)^4$$

The study of the relative stability of the N=0 and the N=1 phases reduces to the comparison of their corresponding free energies  $F_0$  and  $F_1$ .

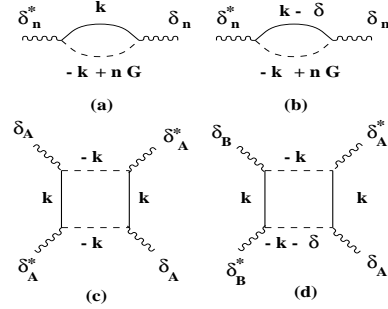


Fig.2: Diagrammatic representation of the second and fourth order terms of the free energy in the N=0 state.  $\delta = \frac{4\Delta}{v_F}$ ,  $\delta_m = I_0 \Delta_0^m$  ( $m=A,B$ ) and  $\delta_n = I_n \Delta_0^{A,(B)}$ .

The second order diagrams (a) and (b) in Fig.2 lead to the instability criterion for the N=0 phase, from which we deduce the  $T_0$  transition temperature.

The coefficients  $b_0$  and  $c_0$  of the fourth order terms in eq.3 are respectively given by (c) and (d) diagrams of Fig.2.  $c_0$  is positive and depends, as  $b_0$  on the effective anion gap  $\Delta$ .

For the N=1 phase, we obtain, as expected, the same Stoner criterion as in the (TMTSF)<sub>2</sub>PF<sub>6</sub> case [5,6]. We denote by  $T_1$  the transition temperature, at which the metallic state is unstable against the formation of the N=1 SDW state.

Close to  $T_0$ , the N=0 phase is semiconducting rather than insulating, because of the small value of the order parameter and of the large thermal fluctuations.

We set  $\Delta_0^A = \Delta_0^B \equiv \Delta_0$ . The minimization of  $F_0$  and  $F_1$ , with respect to  $\Delta_0$  and  $\Delta_1$  shows that  $[F_1]_{\min}$  is lowered compared to  $[F_0]_{\min}$  for  $T < T_1^*$ , where  $T_1^*$  satisfies:  $[F_1]_{\min}(T_1^*) = [F_0]_{\min}(T_1^*)$ .

By decreasing the temperature, the effect of the coupling term in eq.3 gets more and more pronounced, because of the enhancement of the order parameters. However, the latter are still small enough to justify the Landau expansion at low temperature. The N=0 phase is then destabilized and the N=1 phase becomes stable. Hence, at a temperature  $T_1^*$ , a transition from the N=0 phase to the N=1 phase takes place, with a discontinuity of the order parameter. Figure 3 shows the field-temperature phase diagram obtained from Landau calculations. With decreasing temperature, the phase diagram exhibits the presence of two distinct transitions. First, a second order transition occurs at  $T = T_0$  from the metallic state to the N=0 SDW phase. Then, a first order transition takes place at  $T_1^*$  from the N=0 phase to the N=1 phase. According to our calculations  $\Delta_0$  is smaller than  $\Delta_1$  for  $T < T_1^*$ . We therefore suggest that the first order transition is a semiconductor-semiconductor transition, in agreement with the behavior of the magnetoresistance [12,13]. On the other hand, the Hall conductivity in the inner phase is determined by  $\Delta_1$ , in accordance with the experimental results, since, in the case of coexisting order parameters, the Hall conductivity is due the largest

term [25].

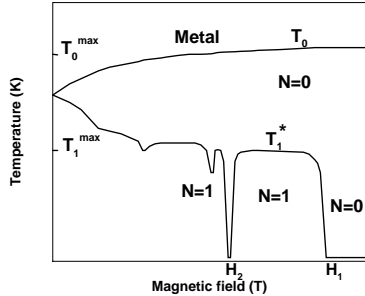


Fig.3: Temperature-field phase diagram of  $(\text{TMTSF})_2\text{ClO}_4$ . The calculations are done for  $E_F = 4000$  K,  $t_1 = 250$  K,  $t_2 = 10$  K,  $V = 8$  K,  $\frac{g_2}{\pi v_F} \sim 0.13$  for the intraband process and  $\frac{g_2}{\pi v_F} \sim 0.17$  for the interband one.  $T_0^{\text{max}} \sim 5.6$  K,  $T_1^{\text{max}} \sim 3$  K,  $H_1 \sim 72$  T and  $H_2 \sim 56$  T.

In the very high field regime, the second order transition line persists, with a nearly field independent critical temperature, while the first order transition temperature decreases strongly and vanishes at  $H = H_1$ . At this critical field and at low temperature, a transition from the  $N=1$  semiconducting state to the  $N=0$  insulating state takes place. At lower field the  $T_1^*$  line collapses at a critical field  $H_2$ . The predicted  $H_1$  and  $H_2$  are higher than the experimental values. However, taking into account the effects of low dimensional fluctuations by using renormalized Landau parameters might still improve the quantitative agreement with the experimental data.

It is important to stress a crucial point: the effective coupling constants  $g_2$  are different for intraband and interband nestings, because of different effects of low dimensional fluctuations [26,27]. Although the bare couplings are, of course, the same, our renormalization group calculation, in the presence of two bands [28] below the anion ordering temperature  $T_{AO}$ , leads to different renormalized couplings for intraband and interband processes. This is an essential feature for the determination of the phase diagram, which, up to now, has been ignored.

On the other hand, for  $H < H_2$ , our proposed phase diagram shows the presence of a new transition line. Chung *et al.* gave recently some arguments in favor of the existence of such line [13]. Furthermore, we found, as expected [3], that the decrease of the imperfect nesting parameter  $t_2$  furthers the formation of  $N=0$  phase.  $H_1$  and  $H_2$  are found to be shifted to lower values. The critical temperature  $T_1^*$  is decreased, whereas  $T_0$  is slightly increased.

In summary, we have proposed a new theoretical phase diagram for  $(\text{TMTSF})_2\text{ClO}_4$  in the high field regime. We have discussed the competition between the high field induced SDW phases. We found that, the  $N=0$  phase has always the highest critical temperature, but it implies the coexistence of two different order parameters, cor-

responding to the two Fermi surfaces. This coexistence tends to destabilize this phase as the temperature is lowered, because of the increase of the order parameters. Eventually, a first order transition occurs, from the  $N=0$  to the  $N=1$  phase. The proposed phase diagram seems to be in qualitative agreement with the experimental data.

We are grateful to J. Moser and D. Jérôme for discussing their unpublished data and we would like to acknowledge N. Dupuis for stimulating discussions.

- 
- [1] C. Bourbonnais and D. Jérôme in advances in Synthetic Metals, Twenty Years of Progress in Sciences and Technology, edited by P. Bernier, S. Lefrant and G. Bidan (Elsevier, New York, 1999), p. 206; D. Jérôme in Organic Conductors : fundamentals and applications, edited by J-P. Farges (Dekker, New York, 1999), p. 405.
  - [2] L. P. Gor'kov and A. G. Lebed, J. Phys. (Paris) Lett. **45**, L433 (1984)
  - [3] M. Héritier, G. Montambaux and P. Lederer, J. Physique Lett. **45**, L943 (1984), M. Héritier, G. Montambaux and P. Lederer, J. Phys. C **19**, L293 (1986)
  - [4] P. M. Chaikin, Phys. Rev. B **31**, 4770 (1985)
  - [5] D. Poilblanc *et al.* J. Phys. C: Solid State Phys. **19**, L321 (1986).
  - [6] A. Virosztek, L. Chen and K. Maki, Phys. Rev. B **34**, 3371 (1986).
  - [7] M. J. Naughton *et al.*, Phys. Rev. Lett. **61**, 621 (1988)
  - [8] W. Kang, S. T. Hannahs and P. M. Chaikin, Phys. Rev. Lett. **70**, 3091 (1993).
  - [9] S. K. McKernan *et al.*, Phys. Rev. Lett. **75**, 1630 (1995)
  - [10] U. M. Scheven *et al.*, Phys. Rev. B **56**, 7804 (1997)
  - [11] S. Uji *et al.*, Phys. Rev. B **55**, 14387 (1997)
  - [12] J. Moser *et al.* unpublished, J. Moser, Ph.D Thesis, Orsay (1999) (unpublished)
  - [13] O-H. Chung *et al.*, Phys. Rev. B **61**, 11649 (2000)
  - [14] S. A. Brazovskii and V. M. Yakovenko, JETP Lett. **43**, 134 (1986)
  - [15] T. Osada, S. Kagoshima and N. Miura, Phys. Rev. Lett. **69**, 1117 (1992)
  - [16] L. P. Gor'kov and A Phys. Rev. B **51**, 3285 (1995).
  - [17] V. M. Yakovenko, Phys. Rev. Lett. **70**, 2657 (1993)
  - [18] J. P. Pouget and S. Ravy, J. Phys. I France **6**, 1501 (1996)
  - [19] J. P. Pouget, J. Phys. IV **10**, Pr3-43 (2000)
  - [20] H. Yoshino *et al.* J. Phys. Soc. Jpn. **66**, 2410 (1997)
  - [21] S. Uji *et al.*, Phys. Rev. B **53**, 14399 (1996)
  - [22] A. G. Lebed, and N. N. Bagmet, Phys. Rev. B **55**, R8654 (1997)
  - [23] T. Osada, S. Kagoshima and N. Miura, Phys. Rev. Lett. **77**, 5261 (1996)
  - [24] Y. Hasegawa, K. Kishigi and M. Miyazaki, J. Phys. Soc. Jpn. **67**, 964 (1998), D. Zanchi and A. Bjeliš, preprint cond-mat/0105530, K. Sengupta and N. Dupuis, Phys. Rev. B **65**, 35108 (2002)
  - [25] V. M. Yakovenko, Phys. Rev. B **43**, 11353 (1991)
  - [26] C. Bourbonnais, private communication

- [27] C. Bourbonnais, *Strongly Interacting Fermions and High  $T_c$  Superconductivity*, p 307. B. Douçot and J. Zinn-Justin, *eds.* Les Houches, Session LVI, 1991
- [28] J. Kishine and K. Yonemitsu, *J. Phys. Soc. Jpn.* **67**, 1714 (1998)